

### 3. Garsia, Ruedy, and Pinkall: Conformal embeddings of closed genus 1 surfaces into $\mathbb{R}^3$

#### 3.1. Preliminaries

Recall that the upper half-plane (UHP) is isomorphic to the Teichmüller space of closed flat tori,  $T(1,0)$ . Tori are parametrized by  $\tau \in \text{UHP}$  so that a parallelogram,  $P_\tau$ , with vertices  $\{0, 1, \tau, \tau+1\}$  and with opposite sides identified, inherits a flat conformal structure. When  $\tau$  is pure imaginary, then  $P_\tau$  is a rectangle and, with opposite sides identified, we refer to it as a *rectangular torus*. The parameter  $\tau$  is called the *modulus* of the torus. Two tori are conformally equivalent precisely when their moduli differ by an action of  $PSL(2, \mathbb{Z})$ , the *modular group*.

There are other ways that, abstractly, a torus can be given a flat metric. The simplest case is just  $S^1 \times S^1$  with the product metric, where we allow the two circles to have different sizes. This abstract flat metric is the same as gluing opposite sides of a Euclidean rectangle whose sides go to circumferences of the circles. There is no isometric embedding of this torus in  $\mathbb{R}^3$ . However, this torus *can* be conformally embedded in  $\mathbb{R}^3$ . Clifford showed this as follows:  $S^1$  embeds in  $\mathbb{R}^2$ . Hence,  $S^1 \times S^1$  embeds in  $\mathbb{R}^2 \times \mathbb{R}^2$ , which is  $\mathbb{R}^4$ . But Clifford showed that no matter what the aspect ratio,  $\tan \rho$ , of the rectangle, this map,  $S^1 \times S^1 \rightarrow \mathbb{R}^4$ ,  $(\theta, \psi, \rho) \mapsto (e^{i(\theta+\psi)} \cos \rho, e^{i\psi} \sin \rho)$ , embeds the torus into  $S^3 \subset \mathbb{R}^4$ . Thus, any rectangular torus embeds isometrically in the 3-sphere. Stereographic projection of  $S^3 \rightarrow \mathbb{R}^3 \cup \{\infty\}$  from the north pole of  $S^3$  to the south polar tangent hyperplane, for example, is accomplished by an inversion of  $\mathbb{R}^4$  in the sphere centered at the north pole of  $S^3$  with radius 2. Thus, stereographically projected images of the Clifford tori in  $\mathbb{R}^3$  are all conformally equivalent to rectangular tori. These conformal images of rectangular

tori are called *cyclides of Dupin*. Pinkall [Pi] applied the Hopf fibration of  $S^3$  to construct conformal embeddings of all closed genus-one Riemann surfaces into  $\mathbb{R}^3$ .

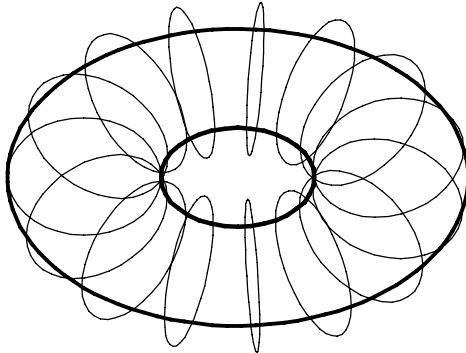
In this chapter we present a new type of conformal embedding of rectangular tori onto tori of revolution in  $\mathbb{R}^3$ . For each rectangular torus, we construct a conformal map that embeds the torus as a closed genus one surface into  $\mathbb{R}^3$ . These constructions are embeddings not only for the rectangular tori, but for all tori that are equivalent to rectangular tori under the action of  $PSL(2, \mathbb{Z})$ .

### 3.1.1. Terminology

Throughout this chapter, we will identify the point  $(x, y)$  with the complex number  $z = x + iy$ . When we refer to the third coordinate in  $\mathbb{R}^3$ , we will use the letter  $t$ , as in  $(x, y, t)$ .

Consider a torus of revolution,  $Q$ , centered at the origin and rotated about the  $t$ -axis. A *latitude* will be any circle on  $Q$  with constant height, that is, with  $t$  equal to a constant. The *outer equator*, respectively *inner equator*, will be the latitude of greatest, respectively least diameter. The generating circles on  $Q$ , the *meridians*, are orthogonal to the latitudes. The latitudes encircle the central hole while the meridians provide the tubular structure of the torus.

(3.1.1.1)



Meridians and the outer and inner equators on  $Q$ .

### 3.2. Main result.

Let  $P = [0, \beta) \times [0, 2\pi)$ . Set  $m = \frac{2\pi}{\beta}$ ,  $\alpha = \frac{-1 + \sqrt{1 + m^2}}{m}$ ,  $R = \frac{\alpha^2 + 1}{2\alpha}$ , and  $\psi = \arg\left(\frac{e^{iy} - \alpha}{1 - \alpha e^{iy}}\right)$ .

Let  $Q$  be the torus of revolution centered at the origin and rotated about the  $t$ -axis with major and minor radii,  $R$  and 1, respectively. Note that with  $\beta \in (0, \infty)$ ,  $R > 1$ , so  $Q$  does not self-intersect. For  $x + iy \in P$ , define the map  $\mathcal{F}$

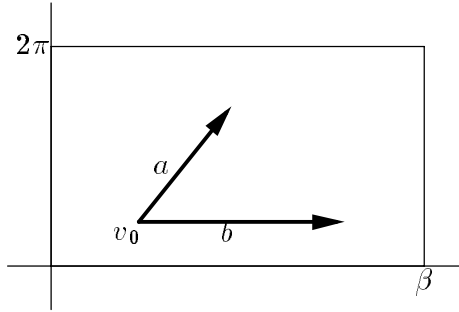
$$\mathcal{F}(x + iy) = \begin{pmatrix} (R + \cos \psi) \cos mx \\ (R + \cos \psi) \sin mx \\ \sin \psi \end{pmatrix}$$

**Theorem 3.2.1.** *For  $\beta \in (0, \infty)$ ,  $\mathcal{F}$  conformally maps the rectangle,  $P = [0, \beta) \times [0, 2\pi)$  onto the torus,  $Q$ .*

We shall need a lemma.

Consider an angle whose edges,  $a$  and  $b$ , and vertex,  $v_0 = (x_0, y_0)$ , all lie in the rectangle  $P$ , which we identify with the tangent plane,  $T_{v_0}P$ .

(3.2.1)



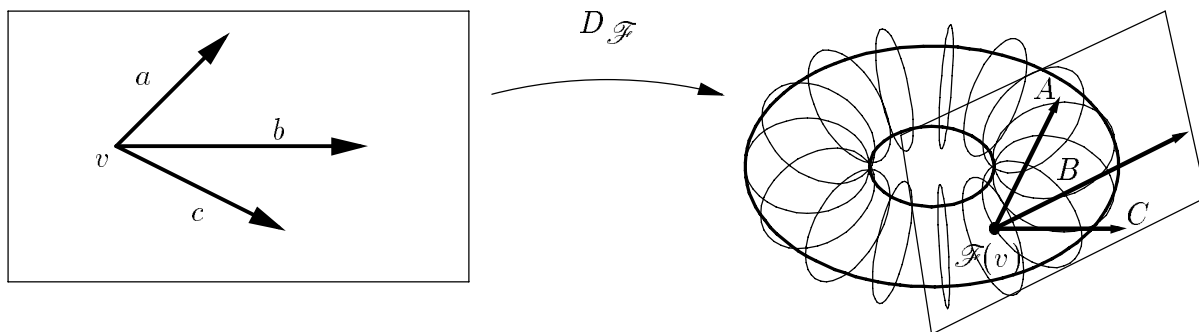
Rectangle with vectors  $a$  and  $b$ .

Computations will be greatly simplified if we may assume that the vector  $b$  lies on the horizontal line through  $v_0$  and points in the positive  $x$ -direction.

**Lemma 3.2.2.** *If  $\mathcal{F}$  preserves the angle between a single fixed vector,  $b$ , based at  $v_0$  and an arbitrary vector,  $a$ , also based at  $v_0$ , then  $\mathcal{F}$  preserves the angle between an arbitrary pair of vectors based at  $v_0$ .*

**Proof.** Denote by  $b$ , a fixed vector based at  $v$  in the tangent space  $T_vP$ . Let  $a$  and  $c$  be arbitrary vectors in  $T_vP$  based at the same point. Let  $D_{\mathcal{F}}(a)$  be the differential map of the function  $\mathcal{F}$  applied to the vector  $a$  at its base point. Now define  $A$  to be  $D_{\mathcal{F}}(a)$  and  $B$  to be  $D_{\mathcal{F}}(b)$ . Let  $\text{angle}(ba)$  denote the angle between vectors  $a$  and  $b$ , counterclockwise from  $b$  to  $a$ . Assume that  $D_{\mathcal{F}}$  preserves the angle between the vectors  $a$  and  $b$  and preserves the angle between vectors  $c$  and  $b$  as well. That is,  $\text{angle}(ba) = \text{angle}(BA)$  and  $\text{angle}(cb) = \text{angle}(CB)$ . Then, our claim is that  $\text{angle}(ca) = \text{angle}(CA)$ . This is true because the vectors are coplanar and the differential map preserves the orientation of vectors.  $\square$  This ends the proof of the lemma.

(3.2.2)



Tangent planes  $T_v P$  and  $T_{\mathcal{F}(v)} Q$ .

We are ready to begin the proof of the theorem.

**Proof:** That the map  $\mathcal{F}$  is a bijection onto  $Q$  will be apparent from the discussion that follows the proof. Let  $v$  be an arbitrary point in the rectangle  $P$ . To prove the conformality of the map  $\mathcal{F}$ , it is sufficient to show that the differential map,  $D_{\mathcal{F}}$ , preserves the angle between vectors in the respective tangent spaces,  $T_v P$  and  $T_{\mathcal{F}(v)} Q$ .

We permanently set  $b(t) = (t + x_0, y_0)$ . Fix  $0 \leq \eta < 2\pi$ . If  $\eta \neq \pm\frac{\pi}{2}$ , then denote  $K = \tan \eta$  and let  $a(t) = (t + x_0, Kt + y_0)$ . If  $\eta = \pm\frac{\pi}{2}$ , then let  $a(t) = (x_0, \pm t + y_0)$ . For convenience, we set  $a = a(\cos \eta)$  and  $b = b(1)$ , unit vectors based at  $v$  and with angle  $\eta$  between them.

We define  $M_\alpha(z) = \frac{z-\alpha}{1-\alpha z}$  and observe that  $\cos \psi + i \sin \psi = M_\alpha(e^{iy})$ . In particular, computing  $\psi$  would be superfluous<sup>8</sup>, since  $\sin \psi$  and  $\cos \psi$  are what we need for our definition of  $\mathcal{F}$ .

---

<sup>8</sup>This key observation eliminates the need for inverse trigonometric functions in the computations for  $\mathcal{F}$  and for  $D_{\mathcal{F}}$ . The use of *Mathematica* symbolic computational subroutines is generally not possible if inverse trigonometric functions are in the expressions.

Some algebra gives us that

$$\cos \psi = \frac{(1 + \alpha^2) \cos y - 2\alpha}{1 + \alpha^2 - 2\alpha \cos y}$$

and

$$\sin \psi = \frac{(1 - \alpha) \sin y}{1 + \alpha^2 - 2\alpha \cos y}.$$

Recall that  $R = \frac{\alpha^2+1}{2\alpha}$ , so we may write  $\mathcal{F}(a(t))$  as

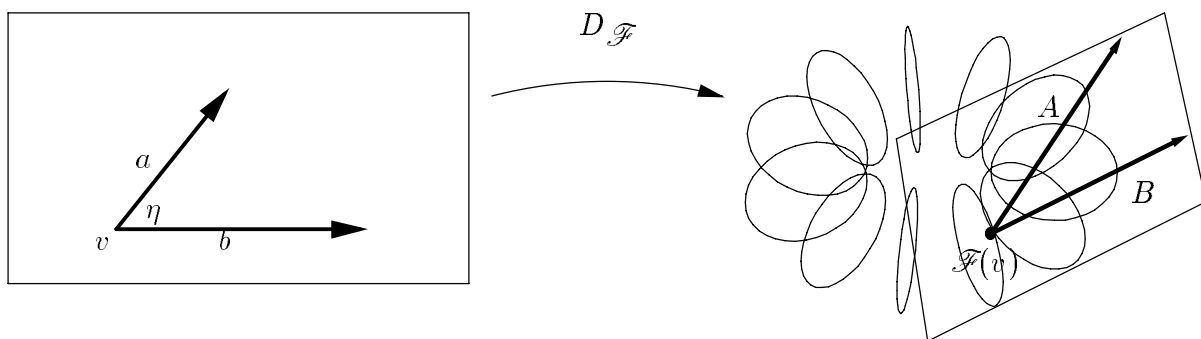
$$\mathcal{F}(t + x_0, Kt + y_0) = \begin{pmatrix} \left( \frac{\alpha^2 + 1}{2\alpha} + \frac{(1 + \alpha^2) \cos(Kt + y_0) - 2\alpha}{1 + \alpha^2 - 2\alpha \cos(Kt + y_0)} \right) \cos\left(\frac{2\pi}{\beta}(t + x_0)\right) \\ \left( \frac{\alpha^2 + 1}{2\alpha} + \frac{(1 + \alpha^2) \cos(Kt + y_0) - 2\alpha}{1 + \alpha^2 - 2\alpha \cos(Kt + y_0)} \right) \sin\left(\frac{2\pi}{\beta}(t + x_0)\right) \\ \frac{(1 - \alpha) \sin(Kt + y_0)}{1 + \alpha^2 - 2\alpha \cos(Kt + y_0)} \end{pmatrix}$$

Denote the images of the vectors  $a$  and  $b$  under the differential map of  $\mathcal{F}$  to be

$$A = D\mathcal{F}(a(t))|_{t=0} \text{ and } B = D\mathcal{F}(b(t))|_{t=0}.$$

Our claim is that the angle between the vectors  $a$  and  $b$  is the same as that between  $A$  and  $B$ . To establish the claim, it is enough to show that  $\frac{A \cdot B}{\|A\| \|B\|} = \frac{a \cdot b}{\|a\| \|b\|} = \cos \eta$ .

(3.2.3)



Angles preserved by the differential map  $D_F$ .

On the next one and one-half pages we show the coordinate expressions computed by *Mathematica* for the vector  $A = D \mathcal{F}(a(t))|_{t=0}$ .

$$\begin{aligned}
A = & \left\{ \frac{\left( \frac{\pi \left( 1 + \frac{(-\beta + \sqrt{\beta^2 + 4\pi^2})^2}{4\pi^2} \right)}{-\beta + \sqrt{\beta^2 + 4\pi^2}} + \frac{-\frac{-\beta + \sqrt{\beta^2 + 4\pi^2}}{\pi} + \left( 1 + \frac{(-\beta + \sqrt{\beta^2 + 4\pi^2})^2}{4\pi^2} \right) \cos(y_0)}{1 + \frac{(-\beta + \sqrt{\beta^2 + 4\pi^2})^2}{4\pi^2} - \frac{(-\beta + \sqrt{\beta^2 + 4\pi^2}) \cos(y_0)}{\pi}}{\beta} \right)}{-2\pi \sin\left(\frac{2\pi x_0}{\beta}\right)} \right. \\
& + \cos\left(\frac{2\pi x_0}{\beta}\right) \left( -\frac{K \left( 1 + \frac{(-\beta + \sqrt{\beta^2 + 4\pi^2})^2}{4\pi^2} \right) \sin(y_0)}{1 + \frac{(-\beta + \sqrt{\beta^2 + 4\pi^2})^2}{4\pi^2} - \frac{(-\beta + \sqrt{\beta^2 + 4\pi^2}) \cos(y_0)}{\pi}} \right. \\
& \left. \left. - \frac{\left( -\frac{-\beta + \sqrt{\beta^2 + 4\pi^2}}{\pi} + \left( 1 + \frac{(-\beta + \sqrt{\beta^2 + 4\pi^2})^2}{4\pi^2} \right) \cos(y_0) \right)}{\pi \left( 1 + \frac{(-\beta + \sqrt{\beta^2 + 4\pi^2})^2}{4\pi^2} - \frac{(-\beta + \sqrt{\beta^2 + 4\pi^2}) \cos(y_0)}{\pi} \right)^2} \right) \right. \\
& \left. \frac{K \sin(y_0) (-\beta + \sqrt{\beta^2 + 4\pi^2})}{\pi \left( 1 + \frac{(-\beta + \sqrt{\beta^2 + 4\pi^2})^2}{4\pi^2} - \frac{(-\beta + \sqrt{\beta^2 + 4\pi^2}) \cos(y_0)}{\pi} \right)^2} \right) \\
& \left. \frac{\left( \frac{\pi \left( 1 + \frac{(-\beta + \sqrt{\beta^2 + 4\pi^2})^2}{4\pi^2} \right)}{-\beta + \sqrt{\beta^2 + 4\pi^2}} + \frac{-\frac{-\beta + \sqrt{\beta^2 + 4\pi^2}}{\pi} + \left( 1 + \frac{(-\beta + \sqrt{\beta^2 + 4\pi^2})^2}{4\pi^2} \right) \cos(y_0)}{1 + \frac{(-\beta + \sqrt{\beta^2 + 4\pi^2})^2}{4\pi^2} - \frac{(-\beta + \sqrt{\beta^2 + 4\pi^2}) \cos(y_0)}{\pi}}{\beta} \right)}{2\pi \cos\left(\frac{2\pi x_0}{\beta}\right)} \right. \\
& + \sin\left(\frac{2\pi x_0}{\beta}\right) \left( -\frac{K \left( 1 + \frac{(-\beta + \sqrt{\beta^2 + 4\pi^2})^2}{4\pi^2} \right) \sin(y_0)}{1 + \frac{(-\beta + \sqrt{\beta^2 + 4\pi^2})^2}{4\pi^2} - \frac{(-\beta + \sqrt{\beta^2 + 4\pi^2}) \cos(y_0)}{\pi}} \right. \\
& \left. \left. - \frac{\left( -\frac{-\beta + \sqrt{\beta^2 + 4\pi^2}}{\pi} + \left( 1 + \frac{(-\beta + \sqrt{\beta^2 + 4\pi^2})^2}{4\pi^2} \right) \cos(y_0) \right)}{\pi \left( 1 + \frac{(-\beta + \sqrt{\beta^2 + 4\pi^2})^2}{4\pi^2} - \frac{(-\beta + \sqrt{\beta^2 + 4\pi^2}) \cos(y_0)}{\pi} \right)^2} \right) \right. \\
& \left. \frac{K \sin(y_0) (-\beta + \sqrt{\beta^2 + 4\pi^2})}{\pi \left( 1 + \frac{(-\beta + \sqrt{\beta^2 + 4\pi^2})^2}{4\pi^2} - \frac{(-\beta + \sqrt{\beta^2 + 4\pi^2}) \cos(y_0)}{\pi} \right)^2} \right) \left. \right\},
\end{aligned}$$

$$\frac{K \left( 1 - \frac{(-\beta + \sqrt{\beta^2 + 4\pi^2})^2}{4\pi^2} \right) \cos(y_0)}{1 + \frac{(-\beta + \sqrt{\beta^2 + 4\pi^2})^2}{4\pi^2} - \frac{(-\beta + \sqrt{\beta^2 + 4\pi^2}) \cos(y_0)}{\pi}} - \frac{K \left( -\beta + \sqrt{\beta^2 + 4\pi^2} \right) \left( 1 - \frac{(-\beta + \sqrt{\beta^2 + 4\pi^2})^2}{4\pi^2} \right) \sin(y_0)^2}{\pi \left( 1 + \frac{(-\beta + \sqrt{\beta^2 + 4\pi^2})^2}{4\pi^2} - \frac{(-\beta + \sqrt{\beta^2 + 4\pi^2}) \cos(y_0)}{\pi} \right)^2}$$

The expressions for  $\frac{A \cdot B}{\|A\| \|B\|}$  are more lengthy and have been left in simplified forms shown in Appendix A, along with the *Mathematica* code that generated the simplifications. Further, we found that the *Mathematica* symbolic computation functions which we used to simplify the expression computed for  $\cos \eta$  give a preference to the form  $\cos 2\theta$  over the expression  $\cos^2 \theta - \sin^2 \theta$ . This created a barrier in the procedure we followed to simplify the expressions. However, once the second expression was forced, then dramatic simplifications were obtained. The *Mathematica* code for the symbolic computations can be found in Appendix A. With the assistance of *Mathematica*, we find that  $\frac{A \cdot B}{\|A\| \|B\|} = \frac{1}{\sqrt{1 + K^2}} = \frac{1}{\sqrt{1 + \tan^2 \eta}} = \cos \eta$ .  $\square$

### 3.3. Background and motivation

#### 3.3.1. Work of Garsia and Ruedy

Garsia proved the existence of conformal embeddings of open Riemann surfaces, i.e., Riemann surfaces with no punctures [G2]. Ruedy extended the result to arbitrary Riemann surfaces [R2]. In an earlier paper, Garsia gave explicit constructions for what he termed *almost conformal* embeddings of closed genus one Riemann surfaces. The construction were “almost” conformal because they failed in conformality only on arbitrarily narrow

neighborhoods about certain “folding” lines. Unfortunately, these constructions reveal little about the shape forced on the genus one surface by the ambient structure of  $\mathbb{R}^3$  and the requirement of conformal equivalence to a given flat torus. On the other hand, Garsia’s constructions, with their composed functions of maps from annuli to spheres, provided motivation for the present work.

In Garsia’s construction, many annuli are mapped to the same sphere. This preserved the conformality of the map at the boundaries of the annuli, but the boundary of the region eventually had to be taken into account. Garsia resolved this difficulty by excluding an arbitrarily narrow neighborhood of the boundary curves wherever different spheres were glued together. Our choice was to lose conformality along many more singular curves on the target surface and to investigate the limiting positions of image points and angles. The action of Möbius transformations on the boundary of the unit disc led us to choose the Möbius transformation  $M_\alpha$ , introduced above, as a likely candidates to deform each meridian on the torus in the required manner.

Pinkall [Pi] constructed conformal embeddings for all closed genus-one Riemann surfaces. However, his constructions rely on the Hopf fibration of  $S^3$ , which cannot be generalized to the higher dimension spaces required for higher genus Riemann surfaces.

### 3.3.2. Normalizations

We normalize the height of our rectangle,  $P$ , to be  $2\pi$ . This is because we apply the exponential function to vertical strips from the rectangle and we wish for the images to be annuli with only their boundaries overlapping. With this normalization,  $P = [0, \beta) \times [0, 2\pi)$  has modulus  $m = \frac{2\pi}{\beta}$ . We also normalize our target tori to have minor radius  $r = 1$ . Note

that such normalizations, accomplished by similarity transformations, have no effect on the conformal structure of these objects.

### 3.3.3. The canonical map $F : \text{rectangle} \rightarrow \text{torus}$

Consider the familiar map  $F : P \rightarrow Q$ , from the rectangle,  $P = [0, \beta) \times [0, 2\pi)$  onto a torus of revolution  $Q \in \mathbb{R}^3$ , given by:

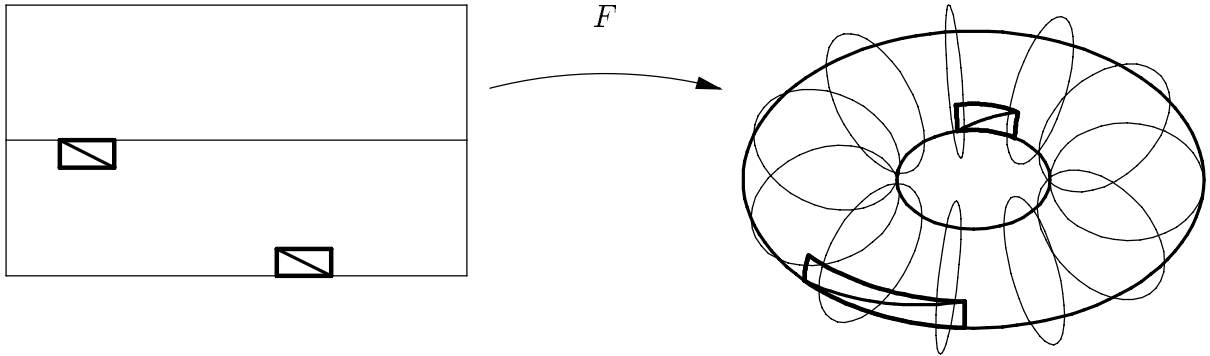
$$(3.3.3.1) \quad F(\phi, \psi) = \begin{pmatrix} (R + \cos \psi) \cos \frac{2\pi}{\beta} \phi \\ (R + \cos \psi) \sin \frac{2\pi}{\beta} \phi \\ \sin \psi \end{pmatrix}; \phi \in [0, \beta), \psi \in [0, 2\pi).$$

The central axis for the torus  $Q = F(P)$  is the  $t$ -axis. The minor and major radii are equal to the real numbers 1 and  $R$ , respectively. The horizontal lines  $\psi = 0$  and  $\psi = 2\pi$  map to the outer equator of  $Q$ . The horizontal line  $\psi = \pi$  maps to  $Q$ 's inner equator.

**Proposition 3.3.3.1.** *The mapping  $F$  is not conformal.*

**Proof.** Consider two small congruent rectangles within the rectangle  $P$ . Let the first be positioned so that its image lies on the torus where the curvature is positive and the other where the curvature is negative.

(3.3.3.2)



Rectangles in  $P$  mapped to  $Q$ .

The vertical edges of the two rectangles will map to equal Euclidean circular arcs, but the horizontal edges will not. Thus, diagonals within the two congruent rectangles will map to arcs that must intersect their respective quadrilateral edges at *different* angles.  $\square$

We shall define a composition function  $F \circ T$  on  $P$  that is conformal onto a torus  $Q$ . Clearly,  $T$  must cause a vertical compression in the map from  $P$  to  $Q$  and the compression must be greatest near the horizontal line in  $P$  which is mapped to the inner equator of  $Q$ , i.e, where the negative curvature of  $Q$  is greatest.

### 3.3.4. Two definitions for the conformal map $\mathcal{F}: P \rightarrow Q$

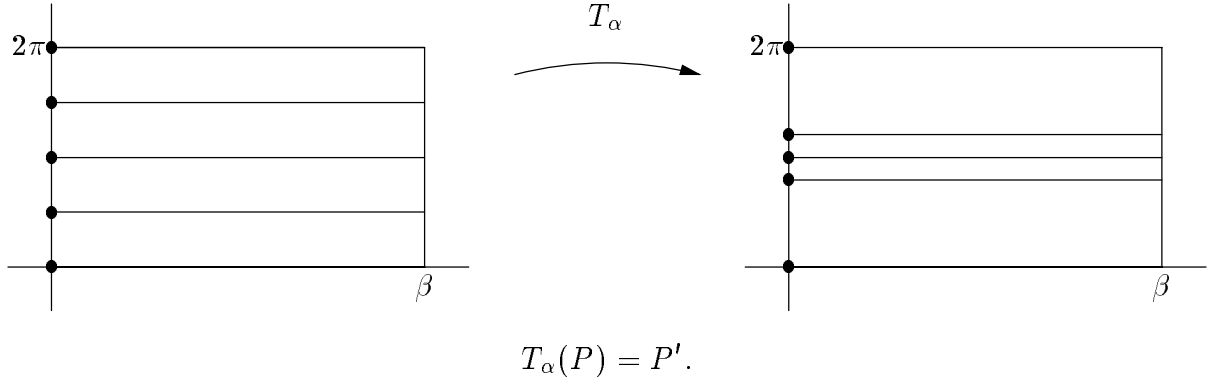
We describe two ways to construct the conformal map  $\mathcal{F}$  in order to provide motivation for our definition. In our first definition we will compose  $F$  with a deformation of the rectangle  $P$ . In our second definition, we will compose a deformation of the torus  $Q$  with the map  $F$ .

Let  $P$  and  $P'$  be the rectangle  $[0, \beta) \times [0, 2\pi)$  in the  $xy$ -, respectively,  $\phi\psi$ -plane. Let  $\alpha \in (0, 1)$ .

We set  $T_\alpha(x, y) = (x, \arg(\frac{e^{iy} - \alpha}{1 - \alpha e^{iy}})) = (\phi, \psi)$ .

**First definition. 3.3.4.1.**  $\mathcal{F}(x, y) = F \circ T_\alpha(x, y)$

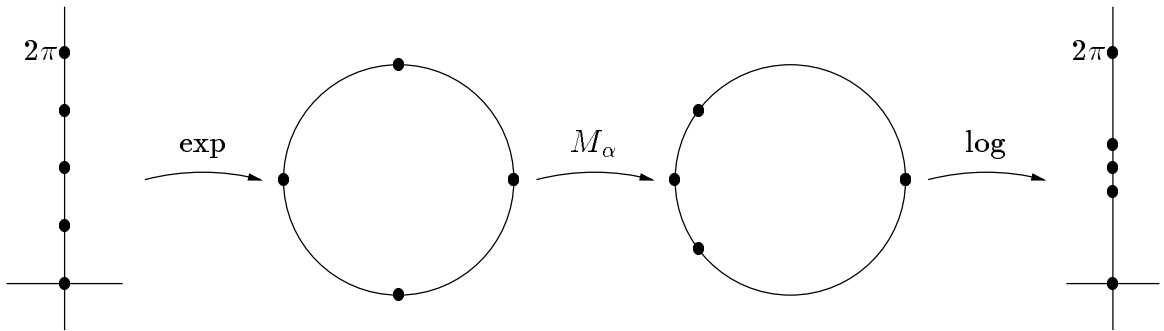
(3.3.4.1)



Note that the family of horizontal lines in  $P$  are preserved. Thus the action of  $T_\alpha$  on the  $y$ -axis determines its action on all of  $P$ . In fact, we let  $M_\alpha(z) = \frac{z-\alpha}{1-\alpha z}$  and note that for  $\psi$  in our definition of  $T_\alpha$ ,

$$i\psi(y) = \log(M_\alpha(e^{iy})).$$

(3.3.4.2)



Action of  $T_\alpha = \log \circ M_\alpha \circ \exp$  on the  $y$ -axis.

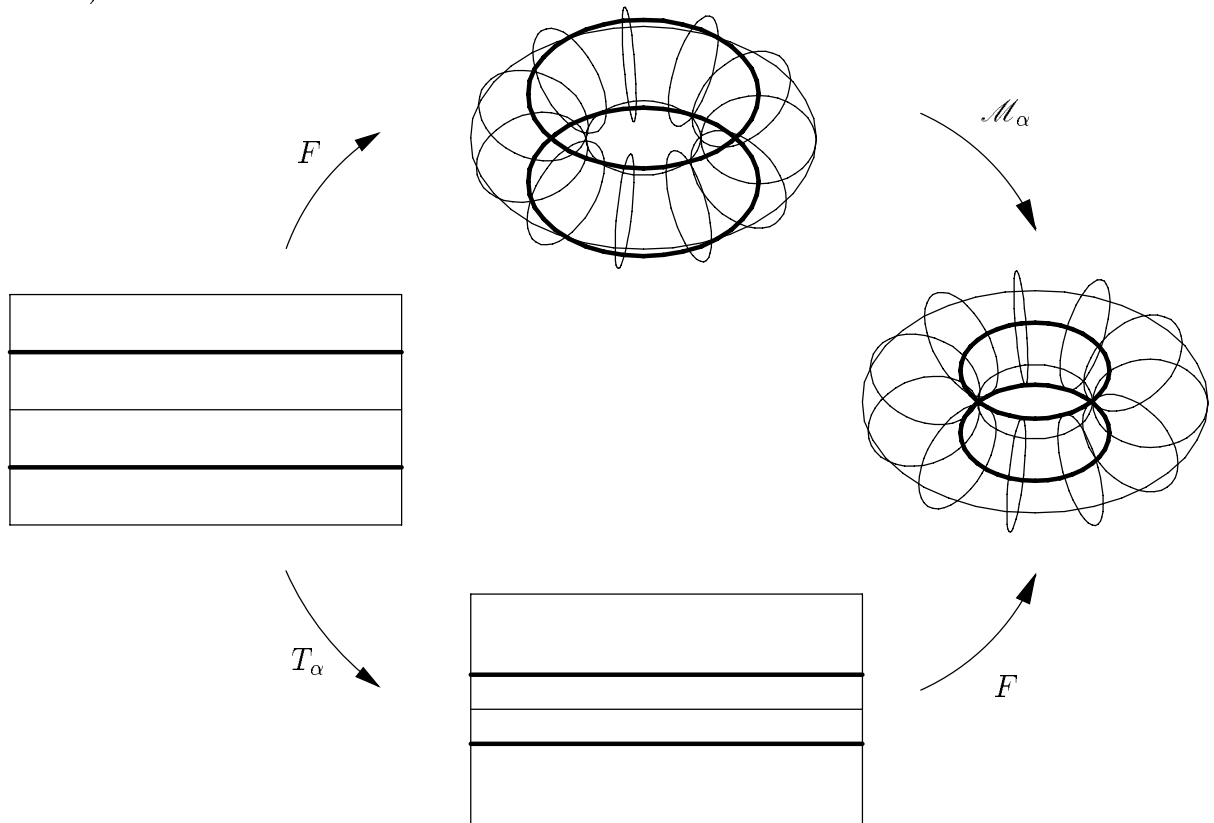
Note that the Möbius transformation,  $M_\alpha$ , preserves the unit circle and displaces points from  $(1, 0)$  towards  $(-1, 0)$ , the attracting fixed point of  $M_\alpha$ . Also note that, since the

attracting point  $(-1, 0)$  corresponds to the inner equator on  $Q$ , that the distortion is, at least qualitatively, what we are seeking.

Let  $\alpha$  be as before, i.e.,  $0 < \alpha < 1$ . Let  $Q$  be the torus as previously described and let  $Q'$  be a torus with the same dimensions. To reparametrize the torus, we define a mapping  $\mathcal{M}_\alpha : Q' \rightarrow Q$  as follows. We identify each meridian of  $Q'$ , in turn, with the unit circle. The intersection of the meridian with the outer equator we identify with the point  $(0, 1) \in \mathbb{C}$  and the intersection with the inner equator, we identify with  $(-1, 0)$ . To this circle we apply the Möbius transformation  $M_\alpha$ . Finally, we translate this circle back to the meridian's original position.

**Second definition. 3.3.4.2.**  $\mathcal{F}(x, y) = \mathcal{M}_\alpha \circ F(x, y)$

(3.3.4.3)



Two alternative definitions of  $\mathcal{F}$ .

It is a simple computation to show that  $F \circ T_\alpha = \mathcal{M}_\alpha \circ F$  on the rectangle  $P$ .

### 3.3.5. Symbolic computations with *Mathematica*

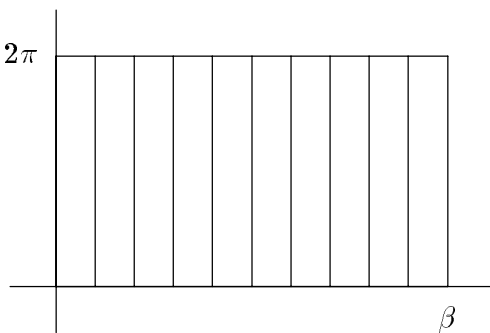
The second definition of  $\mathcal{F}$  emphasizes that the Möbius transformation acts directly on points on the torus meridians. In particular, inverse trigonometric functions need never be used in computing the coordinate functions for  $\mathcal{F}$ . This observation leads to one of the most important features of our function  $\mathcal{F}$ . Although the coordinate functions for  $\mathcal{F}$  do not have simple forms, the absence of inverse functions make them accessible to the symbolic computation subroutines in *Mathematica*.

The following piecewise conformal mapping provides motivation for determining the values for the parameters  $\alpha$  and  $R$ .

### 3.3.6. The piecewise conformal map $F_n$ .

We divide the rectangle,  $P = [0, \beta) \times [0, 2\pi)$  into  $n$  equal vertical strips.

(3.3.6.1)

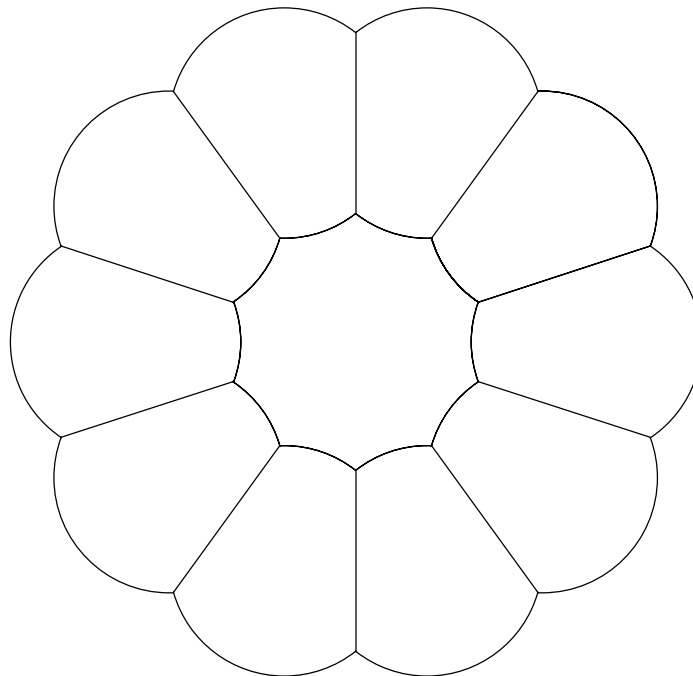


$n$  vertical strips in  $P$ .

We presently will define the map  $F_n$ , a piecewise conformal map on each vertical strip. The image of each vertical strip is a section on a sphere. All  $n$  of these sections are pieced

together to create  $Q_n$ , a piecewise conformal torus. The map  $F_n$  will be conformal except at the boundaries of the vertical strip. These vertical line segments map to the gluing seams on  $Q_n$ .

(3.3.6.2)



Piecewise conformal  $Q_n$ .

The conformality of the map  $F_n$  off the vertical seams will offer us no aid<sup>9</sup> in establishing conformality of a limit function when we let  $n \rightarrow \infty$ ; the seams, where conformality fails, become dense on the rectangle as  $n$  tends towards its limit,  $\infty$ .

The distance from the center of the sphere sections to the central axis of the torus,  $Q_n$ , we will refer to as  $R_n$ . We now define  $F_n$  on each vertical strip.

---

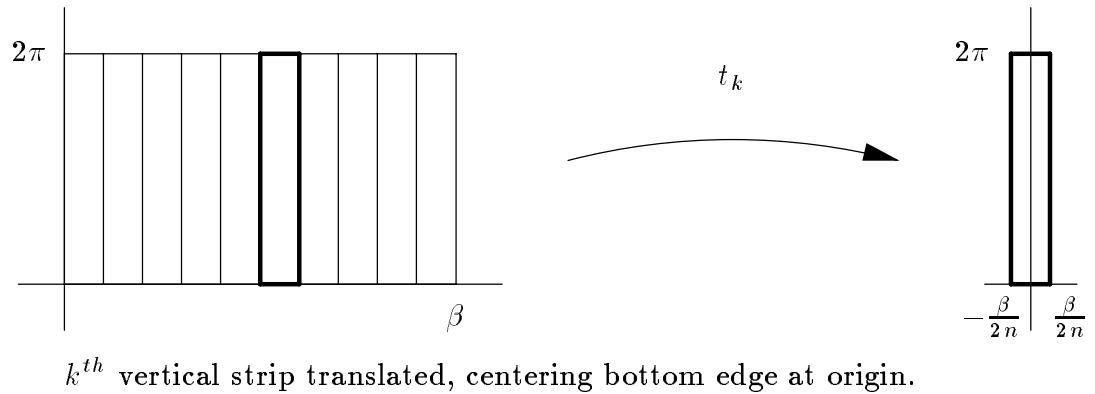
<sup>9</sup>An argument may work which involves the one-sided tangent planes along these seams. The failure of conformality on each seam, in some sense, decreases as  $n \rightarrow \infty$ . The tangent planes converge in the limit along the seams. However, in this work, we have taken a more directly (symbolic) computational route to establish conformality of the limit function.

**Action of  $F_n$  on the  $k^{\text{th}}$  vertical strip in  $P$ .**

Translate the  $k^{\text{th}}$  vertical strip of the rectangle, so that its base is centered at the origin.

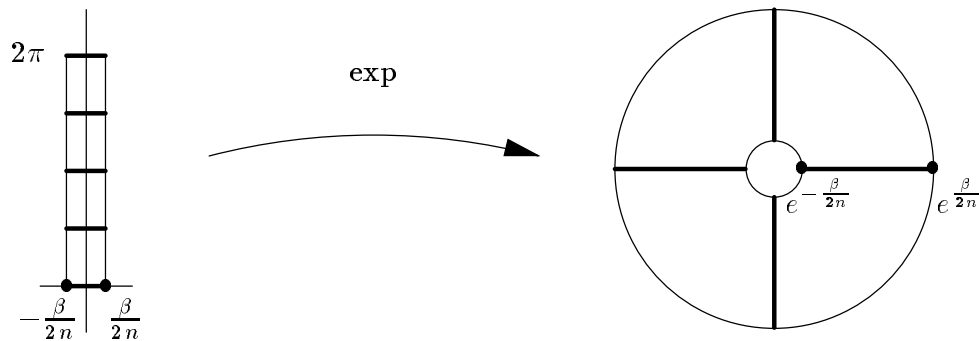
The map is  $t_k(z) = z - \frac{k-\frac{1}{2}}{n}$ .

(3.3.6.3)



Apply the exponential function and obtain an annulus which has as inner and outer boundaries the circles centered at the origin with radius  $e^{-\frac{\beta}{2n}}$  and  $e^{\frac{\beta}{2n}}$ , respectively. Note that each boundary of the annulus is the inversion of the other in the unit circle. This relationship is invariant under Möbius transformations that preserve the unit disc.

(3.3.6.4)

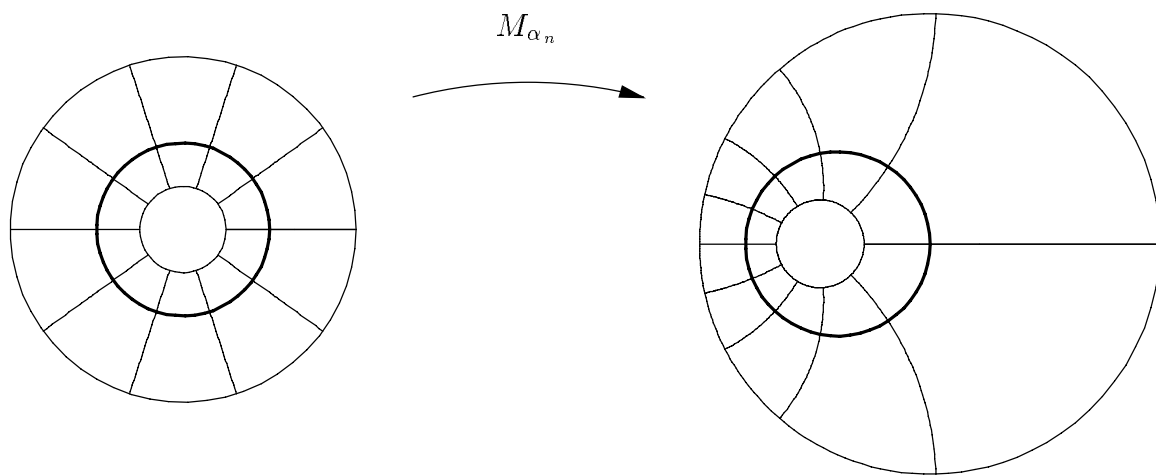


Rectangular strip to annulus.

For  $\alpha_n \in (0, 1)$ , we define  $M_{\alpha_n}(z) = \frac{z-\alpha_n}{1-z\alpha_n}$ . We defer discussion of the value of  $\alpha_n$  until the following section. Its value will be determined by an angle condition imposed by the

model  $Q_n$ . We apply  $M_{\alpha_n}$  to the annulus generated above. The inner, thickened circle in the figure below represents the unit circle.

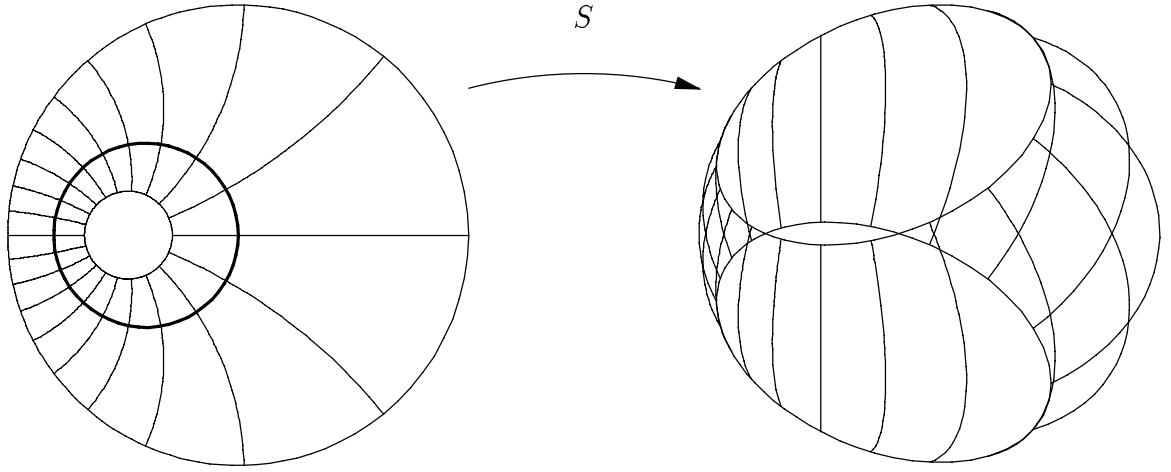
(3.3.6.5)



Action of  $M_{\alpha_n}$  on annulus.

Next we apply the stereographic projection map to the resulting annular region. The image has a profile that looks something like a wedge shaped bead and we refer to it as  $E$ . Since the planar annular region is bounded by circles that are inversions in the unit circle, the region's image has boundaries that are reflections of each other across the  $xy$ -plane. Points on the real axis are those we will consider; for reference, we note that the mapping of these points is  $x + i0 \rightarrow (\frac{2x}{x^2 + 1}, 0, \frac{x^2 - 1}{x^2 + 1})$ . We let stereographic projection of  $z$  be denoted as  $S(z)$ .

(3.3.6.6)



Stereographic projection to the Riemann sphere.

The final step is to position  $E$  so that we may glue all the sections together at their boundaries. We rotate the section an angle of  $\frac{\pi}{2}$  about the  $x$ -axis, translate the distance  $R_n$  (determined by later computations), and finally rotate an angle of  $2\pi \frac{k-1}{n}$  about the  $t$ -axis. We denote these rotations and translation together as  $\rho_k(z)$ .

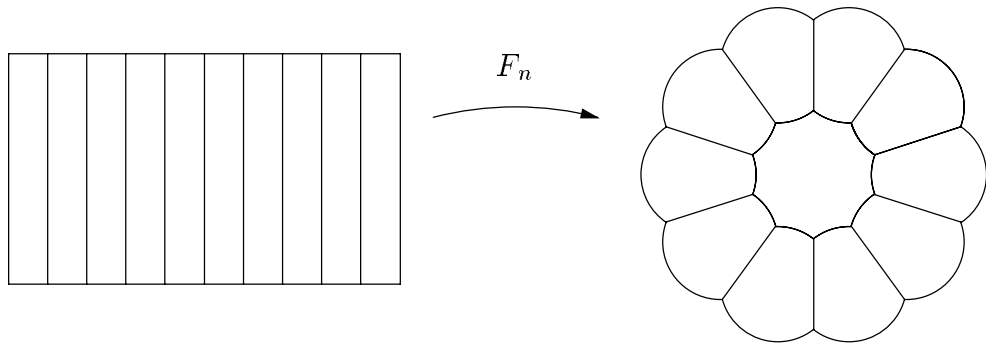
Consider the rectangle  $P$  cut into  $n$  vertical strips and denote the  $k^{\text{th}}$  vertical strip as  $V_k$ . If  $z \in V_k$ , then we define the composition map  $F_n$  to be

$$F_n(z) = \rho_k \circ S \circ M_{\alpha_n} \circ \exp \circ t_k(z).$$

It is clear that the piecewise conformal torus is precisely

$$F_n(P) = \bigoplus_{k=1}^n \rho_k \circ S \circ M_{\alpha_n} \circ \exp \circ t_k(V_k) = Q_n.$$

(3.3.6.7)



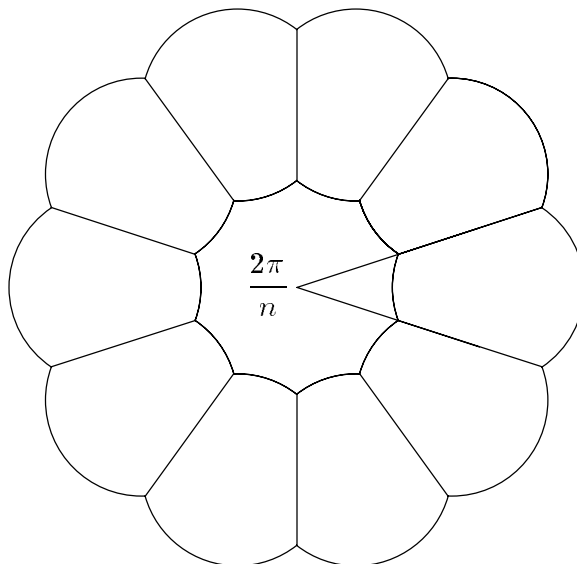
$$F_n(P) = Q_n.$$

### 3.3.7. Determining the parameter $\alpha_n$ .

Let  $\theta$  denote the dihedral angle of the two planes in which the boundary circles of  $E$  lie.

For the  $n$  sphere segments to fit together with no gaps and no overlapping,  $\theta$  must be  $\frac{2\pi}{n}$ .

(3.3.7.1)

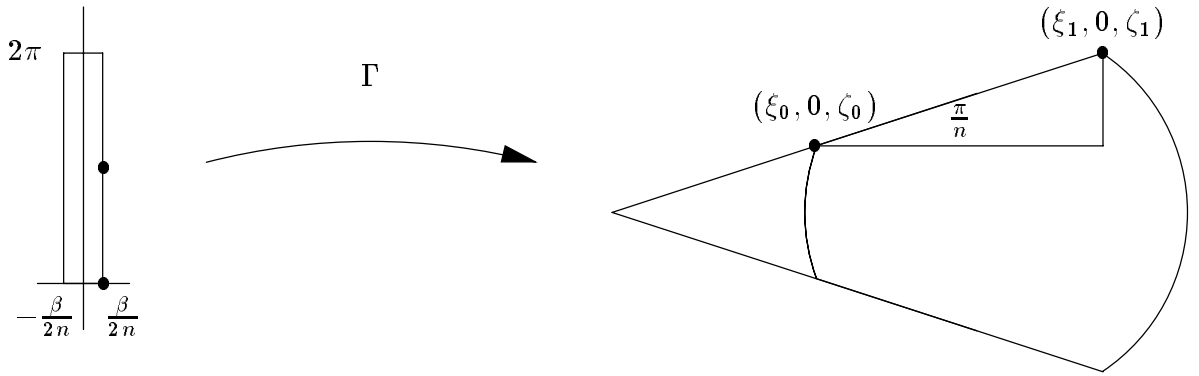


Dihedral angle must be  $\frac{2\pi}{n}$ .

**Lemma 3.3.7.1.** *Given  $\beta \in (0, \infty)$  and  $n \in \mathbb{Z}$ , there exists an  $\alpha_n$  such that the dihedral angle  $= \frac{2\pi}{n}$ . Further,  $\alpha_n = \frac{-\tanh \frac{\beta}{2n} + \sqrt{\tanh^2 \frac{\beta}{2n} + \tan^2 \frac{\pi}{n}}}{\tan \frac{\pi}{n}}$*

**Proof.** We consider a single component of  $Q_n$  before it is rotated and translated into position for gluing, i.e., it is still centered at the origin and is symmetric with respect to the  $xy$ -plane. Viewed from the side, it would look like the figure on the right below. Let  $\Gamma(z)$  be the composition of the exponential map followed by the Möbius transformation  $M_{\alpha_n}$  and then stereographic projection.

(3.3.7.2)



Action of  $\Gamma$  on  $p_1$  and  $p_2$ .

Relationships that hold for points in the figure above are:

$$\Gamma\left(\frac{\beta}{2n}, \pi\right) = (\xi_0, 0, \zeta_0)$$

$$\Gamma\left(\frac{\beta}{2n}, 0\right) = (\xi_1, 0, \zeta_1)$$

In the expressions below we will suppress the subscript  $n$  for the parameter  $\alpha_n$ . The computations for the coordinates are

$$\xi_0 = 2 \frac{\frac{-e^{\frac{\beta}{2n}} - \alpha}{1 + \alpha e^{\frac{\beta}{2n}}}}{\left(\frac{-e^{\frac{\beta}{2n}} - \alpha}{1 + \alpha e^{\frac{\beta}{2n}}}\right)^2 + 1} \quad \zeta_0 = \frac{\left(\frac{-e^{\frac{\beta}{2n}} - \alpha}{1 + \alpha e^{\frac{\beta}{2n}}}\right)^2 - 1}{\left(\frac{-e^{\frac{\beta}{2n}} - \alpha}{1 + \alpha e^{\frac{\beta}{2n}}}\right)^2 + 1}$$

$$\xi_1 = 2 \frac{\frac{e^{\frac{\beta}{2n}} - \alpha}{1 - \alpha e^{\frac{\beta}{2n}}}}{\left(\frac{e^{\frac{\beta}{2n}} - \alpha}{1 - \alpha e^{\frac{\beta}{2n}}}\right)^2 + 1} \quad \zeta_1 = \frac{\left(\frac{e^{\frac{\beta}{2n}} - \alpha}{1 - \alpha e^{\frac{\beta}{2n}}}\right)^2 - 1}{\left(\frac{e^{\frac{\beta}{2n}} - \alpha}{1 - \alpha e^{\frac{\beta}{2n}}}\right)^2 + 1}$$

and, so

$$(3.3.7.3) \quad \tan \frac{\pi}{n} = \frac{\zeta_0 - \zeta_1}{\xi_0 - \xi_1} = \frac{\frac{\left(\frac{-e^{\frac{\beta}{2n}} - \alpha}{1 + \alpha e^{\frac{\beta}{2n}}}\right)^2 - 1}{\left(\frac{-e^{\frac{\beta}{2n}} - \alpha}{1 + \alpha e^{\frac{\beta}{2n}}}\right)^2 + 1} - \frac{\left(\frac{e^{\frac{\beta}{2n}} - \alpha}{1 - \alpha e^{\frac{\beta}{2n}}}\right)^2 - 1}{\left(\frac{e^{\frac{\beta}{2n}} - \alpha}{1 - \alpha e^{\frac{\beta}{2n}}}\right)^2 + 1}}{2 \frac{\frac{-e^{\frac{\beta}{2n}} - \alpha}{1 + \alpha e^{\frac{\beta}{2n}}}}{\left(\frac{-e^{\frac{\beta}{2n}} - \alpha}{1 + \alpha e^{\frac{\beta}{2n}}}\right)^2 + 1} - 2 \frac{\frac{e^{\frac{\beta}{2n}} - \alpha}{1 - \alpha e^{\frac{\beta}{2n}}}}{\left(\frac{e^{\frac{\beta}{2n}} - \alpha}{1 - \alpha e^{\frac{\beta}{2n}}}\right)^2 + 1}}.$$

With assistance<sup>10</sup> from *Mathematica*, we find the following equivalent and surprisingly simple equation.

$$\tan \frac{\pi}{n} = \frac{2\alpha(e^{\frac{\beta}{n}} - 1)}{(e^{\frac{\beta}{n}} + 1)(1 - \alpha^2)}$$

With the recognition that  $\tanh \frac{\beta}{2n} = \frac{e^{\frac{\beta}{n}} - 1}{e^{\frac{\beta}{n}} + 1}$ , we obtain

$$(3.3.7.4) \quad \tan \frac{\pi}{n} = \frac{2\alpha \tanh \frac{\beta}{2n}}{1 - \alpha^2}.$$

We bring back the subscript  $n$  for  $\alpha$  and we find two roots for  $\alpha_n$ , but only one root has magnitude less than 1, a condition set for the parameter of  $M_{\alpha_n}$ . Considering only the positive root for  $\alpha_n$ , we get

$$(3.3.7.5) \quad \alpha_n = \frac{-\tanh \frac{\beta}{2n} + \sqrt{\tanh^2 \frac{\beta}{2n} + \tan^2 \frac{\pi}{n}}}{\tan \frac{\pi}{n}}$$

This was our claim.  $\square$

---

<sup>10</sup>For the *Mathematica* code, see appendix B.

### 3.3.8. Extensions of $M \in PSL(2, \mathbb{C})$ and of stereographic projection into all of $\mathbb{R}^3$

We make use of the fact that the usual stereographic projection is actually the restriction of a sphere inversion. See, for instance, [N, p142] or [S1, pp52-54.] Let  $\mathcal{S}$  denote the inversion of  $\mathbb{R}^3 \cup \{\infty\} = S^3$  in the sphere with radius  $\sqrt{2}$  centered at  $(0, 0, 1)$ . It is a simple computation to establish that  $\mathcal{S}|_{\mathbb{C} \cup \{\infty\}}$  agrees with stereographic projection from the extended plane to the Riemann sphere, with  $\infty$  mapped to  $(0, 0, 1)$ .

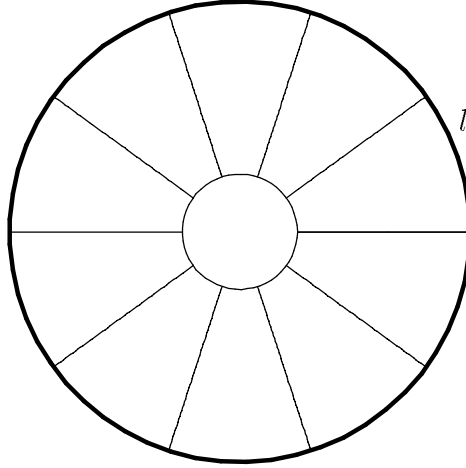
We know that we can extend any Möbius transformation acting on  $\mathbb{C} \cup \{\infty\}$  into the upper half-space via the Poincaré extension and, reflecting in the  $xy$ -plane, extend it into all of  $\mathbb{R}^3$ . Using these two extensions into  $\mathbb{R}^3$  will allow us to consider auxiliary lines and planes in our constructions. When we apply stereographic projection to  $\mathbb{C}$ , we consider certain tangent and bounding spheres that do not coincide with  $\mathbb{C}$ . The action of the functions  $\mathcal{S}$  and extended Möbius transformations on these spheres will guide some of our computations.

### 3.3.9. The action of the extended functions on auxiliary circles and spheres

We wish to better understand the relationships between  $\alpha_n$ ,  $R_n$ , and the dihedral angle  $\frac{2\pi}{n}$ . Towards this end we consider a number of auxiliary circles and spheres. Throughout this section, we replace stereographic projection with the involution  $\mathcal{S}$ , the inversion in the sphere centered at  $(0, 0, 1)$  with radius  $\sqrt{2}$ . We also mean for  $M_\alpha$  to be viewed as its Poincaré extension into all of  $\mathbb{R}^3$ . We will be especially interested in the action of the extended functions,  $\mathcal{S}$  and  $M_\alpha$ , on two circles. The first circle is the outer boundary of the annulus obtained when we applied the exponential function to one of the vertical strips in

$P$ . We will refer to this circle as  $l$ .

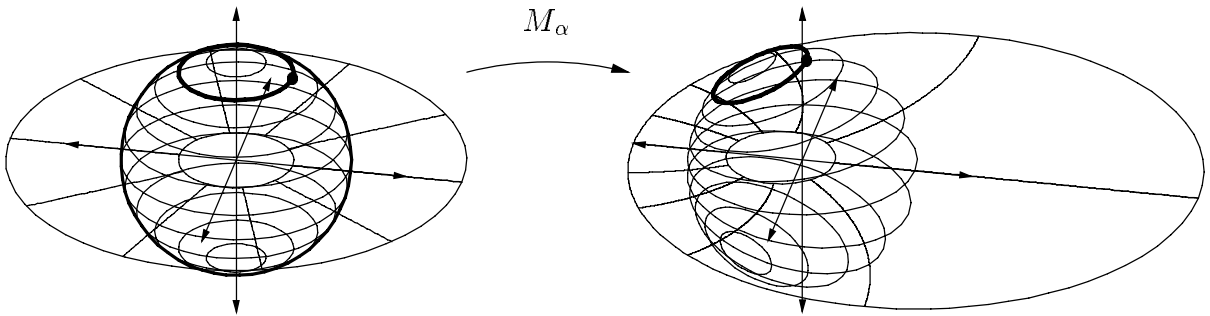
(3.3.9.1)



The outer boundary of the annulus is the circle  $l$ .

The second circle lies on the unit sphere and we will call it  $l_\alpha$  because its position depends on our choice of the parameter  $\alpha$ . We note that, since  $M_\alpha|_{\mathbb{C}}$  preserves the unit circle, the Poincaré extension preserves the unit sphere. Once  $\alpha$  is chosen, we find  $p$ , the pre-image of the north pole, i.e.,  $p = M_\alpha^{-1}(0, 0, 1)$ . The circle  $l_\alpha$  will be the latitude on the unit sphere that passes through  $p$ . The circle  $l_\alpha$  is depicted in the figure below by the thickened latitude on the sphere. Apparently,  $M_\alpha(l_\alpha)$  is a circle passing through the sphere's north pole.

(3.3.9.2)



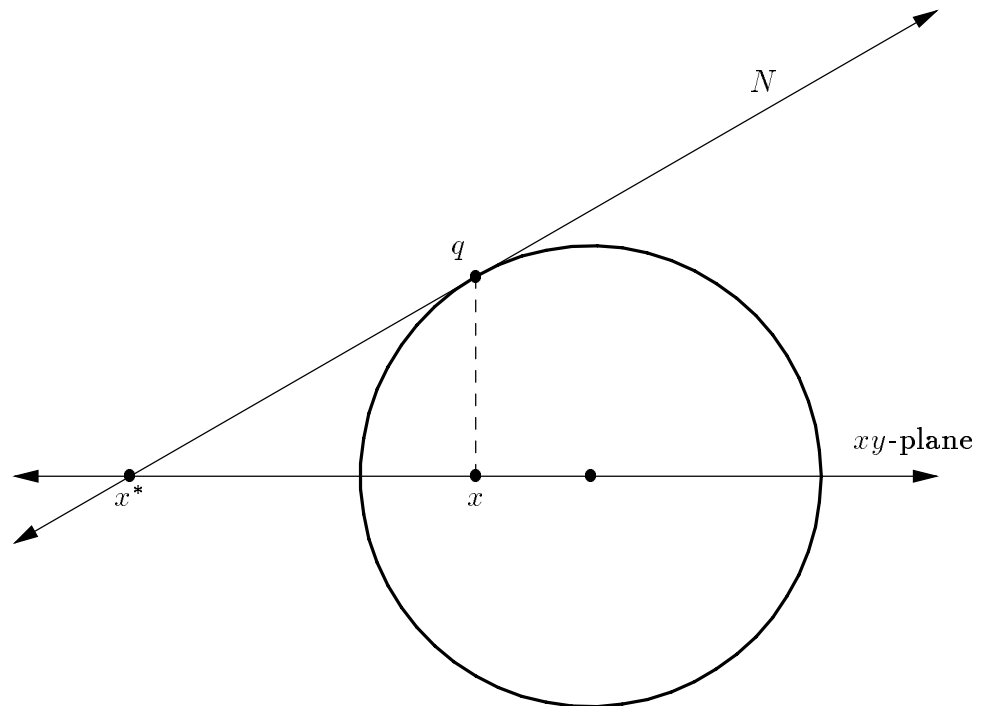
Action of the Poincaré extension of  $M_\alpha$  on the sphere and on the annulus in the plane.

The image of  $p$  is infinite, i.e.,  $\mathcal{S}(M_\alpha(p)) = \infty$ . Thus, the image of the circle,  $l_\alpha$ , is a line lying in  $\mathbb{C}$ . In fact, the image  $L_\alpha = M_\alpha(l_\alpha)$  lies in the same position, relative to the sphere wedge,  $E$ , as does the axis of symmetry of  $Q_n$ , relative to one of the sections of  $Q_n$ . For convenience we will refer to  $L_\alpha$  as the axis of symmetry for  $Q_n$ . Each plane passing through  $L_\alpha$  will be the image of a sphere passing through the latitude circle  $l_\alpha$ . We will want to follow the action on the unique sphere that passes through both circles,  $l_\alpha$  and  $l$ . The image of this sphere will be a plane passing through the line  $L_\alpha$  (axis of symmetry) and through the boundary circle of the wedge shaped sphere segment,  $E$ . This boundary circle corresponds to one of the gluing seams of  $Q_n$ . These circles and the sphere passing through them provide a way to see intuitively that, no matter how narrow the vertical strips become, there will always be an  $\alpha$  such that the dihedral angle of the section  $E$  will be precisely  $\frac{2\pi}{n}$ , the required angle for gluing. The width of the vertical strip determines the diameter of the circle  $l$ . This circle will be mapped to the boundary circle of  $E$ . By varying the value of  $\alpha$ , we change the height of the latitude  $l_\alpha$ . This, in turn, changes the position of  $L_\alpha$ , located a distance  $R_\alpha$  from the origin, and changes the pitch of the plane through  $\mathcal{S}(M_\alpha(l))$ , which is the boundary of the sphere section  $E$ . The continuous change in height of  $l_\alpha$ , results in a continuous change in the dihedral angle of the plane through  $\mathcal{S}(M_\alpha(l))$  and the  $xy$ -plane. It is clear that we can obtain any dihedral angle measure from zero to  $\frac{\pi}{2}$  by an appropriate choice of height for the circle  $l_\alpha$  on the sphere.

There is one other plane through  $L_\alpha$  that interests us: the plane tangent to the unit upper hemisphere. This plane, which we will denote by  $N$ , will be the image of the sphere which is tangent to the  $xy$ -plane and which passes through the circle  $l_\alpha$ . By symmetry, the point of tangency for the sphere through  $l_\alpha$  is the origin. Thus, the point of tangency,  $q$ ,

for  $N$  on the unit sphere is the image of the origin, i.e.,  $q = \mathcal{S} \circ M_\alpha(0, 0, 0)$ . Let  $z^* = \frac{1}{z}$ , that is,  $z^*$  is the inversion of a complex number over the unit circle. The intersection of the  $xt$ -plane with the unit sphere and the plane  $N$  contains an illustration for the classic construction of inverse points over the unit circle. The relationship that holds for the  $x$ -coordinants in the illustration below is  $x \cdot x^* = 1$ .

(3.3.9.3)



$$x \cdot x^* = 1.$$

The value for  $|x^*|$  is the length  $R_n$ , the radial distance of  $Q_n$ . Since the  $x$ -component of  $\mathcal{S} \circ M_\alpha(0, 0, 0)$  is  $\frac{-2\alpha_n}{1+\alpha_n^2}$ , we have  $R_n = \frac{1+\alpha_n^2}{2\alpha_n}$ .

### 3.3.10. Computations for $\alpha$ and $R$ , parameters for $\mathcal{F}$ , as limits

From lemma 3.2.2.1, we have that a value  $\alpha_n$  exists that allows the construction of the piecewise conformal torus  $Q_n$ . What happens when we allow  $n \rightarrow \infty$ ? Considering the

relevant Maclaurin series, or with a simple application of L'Hopital's rule, if you prefer, we get

$$(3.3.10.1) \quad \lim_{n \rightarrow \infty} \alpha_n = \frac{-\beta + \sqrt{\beta^2 + 4\pi^2}}{2\pi} = \frac{-1 + \sqrt{1 + m^2}}{m},$$

where  $m = \frac{2\pi}{\beta}$ , the modulus of the rectangle  $P$ .

$$\text{Finally, } R = \lim_{n \rightarrow \infty} R_n = \frac{\alpha^2 + 1}{2\alpha}$$

Note that as the rectangle becomes long and relatively skinny (as  $m$  decreases), the torus becomes increasingly skinny itself. The major radius,  $R$ , increases while the minor radius remains fixed at 1. On the other hand, with short base lengths the rectangle maps onto a torus the shape of a very fat tire. Since the rectangles with base lengths  $\beta$  and  $\frac{1}{\beta}$  are similar and we view them as equivalent Riemann surfaces, a Riemann surface can be seen as skinny from one point of view and fat from another.